A high sensitivity open loop electronics for gravimetric acoustic wave-based sensors

D. Rabus[1], J.-M. Friedt[2], S. Ballandras[1,2], G. Martin[1], É. Carry[1], and V. Blondeau-Patissier[1]

[1]FEMTO-ST, Université de Franche-Comté, UMR CNRS 6174, 26 chemin de l'épitaphe, 25030 Besançon, FRANCE
[2]SENSEOR, Temis Innovation, 18 rue Alain Savary, 25000 Besançon, FRANCE

March 11, 2013

Abstract: Detecting chemical species in gas phase has recently received an increasing interest mainly for security control, trying to implement new systems allowing for extended dynamics and reactivity. In this work, an open-loop interrogation strategy is proposed to use radio-frequency acoustic transducers as micro-balances in that purpose. The resulting system is dedicated to the monitoring of chemical compounds in gaseous or liquid phase state. A 16 Hz standard deviation is demonstrated at 125 MHz, with a working frequency band in the 60 to 133 MHz range, answering the requirements for using Rayleigh and Love-wave-based delay lines operating with 40 μm acoustic wavelength transducers. Moreover this electronic set-up was used to interrogate High overtone Bulk Acoustic wave Resonator (HBAR) microbalance, a new sensor class allowing for multi-mode interrogation for gravimetric measurement improvement. The noise source still limiting the system performance is due to the Analog-to-Digital Converter of the microcontroller, thus leaving open degrees-of-freedom for improving the obtained results by optimizing the voltage reference and board layout. The operation of the system is illustrated using a calibrated galvanic deposition at the surface of Love-wave delay-lines to assess theoretical predictions of their gravimetric sensitivity and to compare them with HBAR based sensor sensitivity.

1 Introduction

Current systems for detecting potentially toxic gases are in general cumbersome and complex. For continuous, real time monitoring, direct detection sensors are well-adapted as they do not require preliminary sample processing: optical [1], electrochemical [2] or gravimetric acoustic sensors (better known as micro-balances) [3] have been developed and successfully tested for such purposes. Most of the literature references focuses on improving the transduction principle [4, 5, 6], either by replacing propagating waves with evanescent waves which, by being confined close to the transducer surface, improve the signal to noise ratio (Surface Plasmon Resonance – SPR – and Love mode surface acoustic wave sensors – SAW – sensors). In this work, the effort is oriented toward the development of an embedded electronics for gaseous chemical species detection using radio-frequency (RF) transducers. One of the aspects of this dedicated application is the ability to automatically identify an optimal operating frequency point within the pass band of the device, and then to generate a clean, continuous wave signal at this given frequency, with sub-hertz resolution.

The basic principle of gravimetric acoustic wave sensors consists in the measurement of the phase velocity variations due to an adsorbed mass or a layer thickness change atop the device during chemical reaction: this phase velocity is dependent on the boundary conditions of the propagating surface acoustic waves and is affected either by the guiding layer properties or its thickness. A usual principle exploits bulk acoustic waves, yielding the well-known concept of Quartz Crystal Microbalance (QCM) [7]. The gravimetric sensitivity of the QCM is directly related to its thickness and as a consequence to its fundamental frequency f_0. Particle deposition on one side of the resonator modifies its resonance conditions and thus allows for a gravimetric detection. Furthermore, it is possible to functionalize the surface with specific reactants to provide information on the concentration of the adsorbed (target) species in the medium surrounding the sensor [8].

In this work, the development of a dedicated embedded instrument is proposed, based on a full software control for the open-loop monitoring of delay lines. As opposed to the closed-loop – oscillator – strategy which performance is strongly depending on the environment of the acoustic transducer and might yield to a lack of oscillation if the damping of the acoustic waves is not compensated for by the amplifier, an open-loop strategy provides, beyond the actual acoustic parameters, the data needed for measurement even using a poorly performing transducer. Indeed, in an open-loop strategy, the large dynamic range (DC to 2.7 GHz) of the In-phase/Quadrature of phase (I/Q) demodulator needed to extract the phase and magnitude information at each frequency yields improved robustness of the measurement system – transducer and associated electronics – in regard with the closed-loop strategy [3]. However, reaching comparable noise levels with the former strategy is challenging. As a consequence, an embedded frequency-sweep network analyzer has been developed and optimized to meet these specifications, based on a high stability frequency source to synthesize the frequency scanning signals.

In that purpose, a Direct Digital Synthesizer (DDS)-based oscillator is implemented to provide a flexible RF probe signal, while a low noise phase detector is fed by an amplitude-controlled signal. This low noise electronics is used in parallel with a versatile wide-band I/Q demodulator for the preliminary characterization of the transfer function of any type of sensor and for selecting the optimum operating frequency used throughout the gravimetric detection experiment.

The first part of the paper describes the basic principles of the interrogation, in particular the RF signal synthesis and the proposed approach for detection resolution improvement. The resulting electronic set-up is used for calibrating Love-wave devices using an electro-deposition process, allowing for an accurate control of the amount of material deposited atop the device. Finally, a new class of sensors based on High overtone Bulk Acoustic wave Resonator (HBAR) is tested using the developed equipment.

2 Basic principles

2.1 Radio-frequency signal controls

Probing gravimetric acoustic wave-based sensors need to synthetize RF signals: the working frequency is within the 60-133 MHz range, consistent with the use of 40 μm wavelength Rayleigh wave or Love mode surface acoustic wave sensors. The RF probe signal is generated by an Analog Devices AD9954 Direct Digital Synthesizer, controlled by an ARM7-core based ADuC7026 microcontroller through the SPI (Serial Peripheral Interface) link. In order to perform differential measurements, two transducers are probed simultaneously, one coated with a sensing layer and the other one kept free as a reference. Since the two devices exhibit different working conditions, either due to manufacturing differences or due to the sensing layer coating, the probing signals have to be generated by two independent DDS. Each RF signal is split into a reference channel and a measurement line. A programmable attenuator is tuned to generate an output signal of the reference line exhibiting a power close to the signal going through the measurement line.

A coarse measurement mode uses an integrated I/Q demodulator (Fig.1) – Analog Device's AD8302 – with a large bandwidth yielding a standard deviation of 0.3^o on the phase detection output, consistent with the performance of most frequency-sweep RF network analyzers, providing an output similar to the S_{21} parameter classically used to characterize SAW delay lines.

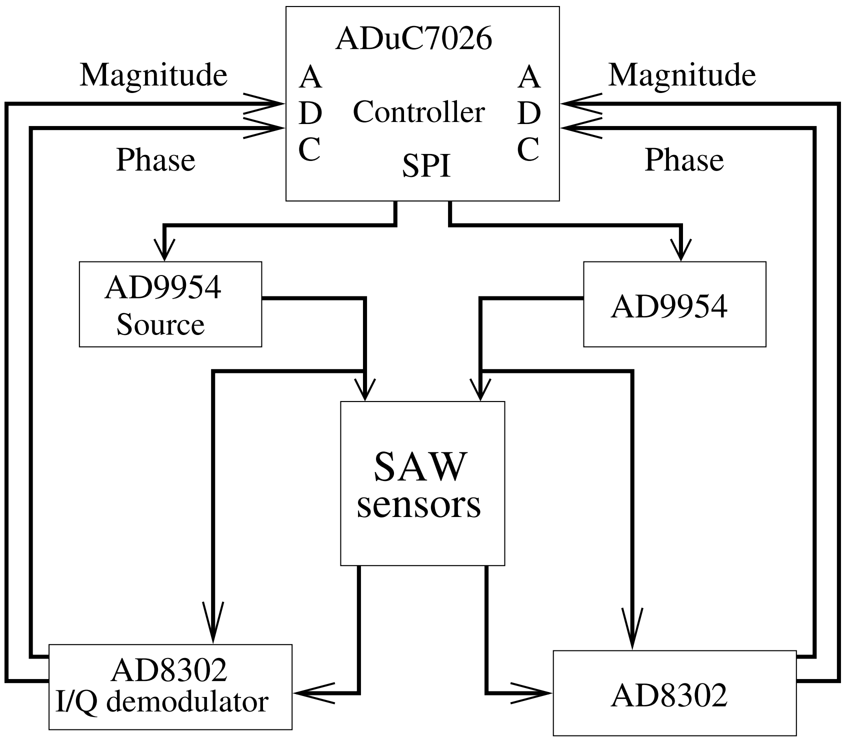

Figure 1: General diagram of two SAW sensors probing electronics, including an ADuC7026 microcontroller, AD9954 Direct Digital Synthesizer, and AD8302 I/Q demodulator.

The setpoint – selection of the frequency at which all measurements will be performed during the chemical reaction – is computed once a full-band (100 to 150 MHz) frequency sweep has been achieved, allowing for the identification of the maximum transmitted signal, max($|S_{21}|$). Identifying this setpoint, the closest mid-scale crossing condition of the S_{21} phase is seeked for, at which the I/Q demodulator exhibits the strongest linearity characteristic the analog-to-digital converter provides the widest dynamic range. Once the operating frequency finely tuned, this setpoint is used throughout the chemical reaction monitoring, and the evolution of magnitude and phase of the I/Q demodulator output is recorded as a function of time.

Due to the noise level (associated with the large bandwidth 30 MHz inducing excessive thermal noise) of the AD8302 demodulator, this coarse scanning approach had to be improved for more accurate measurement by adding a manual phase-detection process – using the SYPD-2 phase detector by Mini Circuits – with an automatic gain controller – Analog Devices AD8367 – wich provides a constant RF signal power from the SAW sensor to the phase measurement by SYPD-2 device. The phase detector is completed with programmable, high-gain low-noise operational amplifiers for signal shaping. This low-bandwidth (143 kHz cutoff frequency) circuit exhibits a noise level small enough for the signal-to-noise ratio to be independent on the operational amplifier stage gain, but limited by the phase velocity fluctuations of the SAW delay line due to operating condition variations.

A second limitation is induced from the DDS synthetiser whose phase noise is about -115±5 dBc/Hz. The phase variation due to the syntethetiser phase noise can be calculated using equation (1) deduced from equation (2) [9].

$$\Delta\varphi_{rms} = \sqrt{2 \times 10^{\frac{L_c(f)}{10}} \times BW} \tag{1}$$

with $\Delta\varphi_{rms}$ the phase variation in radian, L_c the phase noise and BW the bandwidth.

$$L_c(f) = 10 \times \log\left(\frac{1}{2} \times S_{\Delta\varphi}(f)\right) = 10 \times \log\left(\frac{1}{2} \times \frac{\Delta\varphi_{rms}^2}{BW}\right) \tag{2}$$

with $S_{\Delta\varphi}(f)$ the ratio of the noise power measured in a sideband over a bandwidth of 1 Hz to the carrier power. The bandwidth is determined by the cut off frequency of the low pass filter (143 kHz) yielding a phase variation due to the synthetiser of about $\sqrt{2.10^{-120/10} \times 143.10^3}$=30 m^o.

The phase measurement is averaged over 16 samples, yielding a reduction by a factor of $\sqrt{16} = 4$ of the phase noise and thus a phase variation of 7.5 m^o close to the observed 8.2 m^o phase measurement standard deviation when using a 17.4 gain value of the low noise amplifier (Table 1).

The programmable gain of the amplifiers is set using an analog multiplexer. All setpoint identification and gain control tasks are controlled by the same ADuC7026 microcontroller.

The main issue when increasing the gain after the low-noise phase-detection circuit is the limited working range of the phase detection range: since the 0-180^o range no longer fits on phase domain the analog-to-digital converter voltage range, saturation occurs for large mass variations yielding large acoustic velocity shifts. Hence, a phase tracking and unwrapping strategy is implemented, as discussed in section 3.

2.2 S_{21} parameter measurement

2.2.1 Coarse measurement

For preliminary characterization of the delay line, the AD8302 I/Q demodulator provides a magnitude output of 29 mV/dB and a phase output of 10 mV per degree, the latter exhibiting a poor linearity close to the measurement boundaries (0 and 180^o). The frequency selection strategy focuses on selecting a setpoint at which the reference and measurement signals are in quadrature, yielding the best dynamic range and linearity of the output voltage with respect to the phase between the input reference and measurement signals. Figure 3 shows a typical S_{21} characterization of a Love-mode SAW delay line performed with the developed set-up, in the 120 to 130 MHz range and a characterization using commercial network analyser.

2.2.2 Improved accuracy

In order to improve the phase measurement resolution, a low-bandwidth phase detector is associated with low-noise amplifiers. The phase detector provides a low voltage *vs* phase coefficient – 8 mV per degree – but with a noise level low enough to be amplified with a substantial gain as discussed before.

Using variable gain amplifiers, the S_{21} phase characterization of SAW delay line phase behavior is a function of frequency (by a frequency sweep) with gains ranging from 1 to 16:

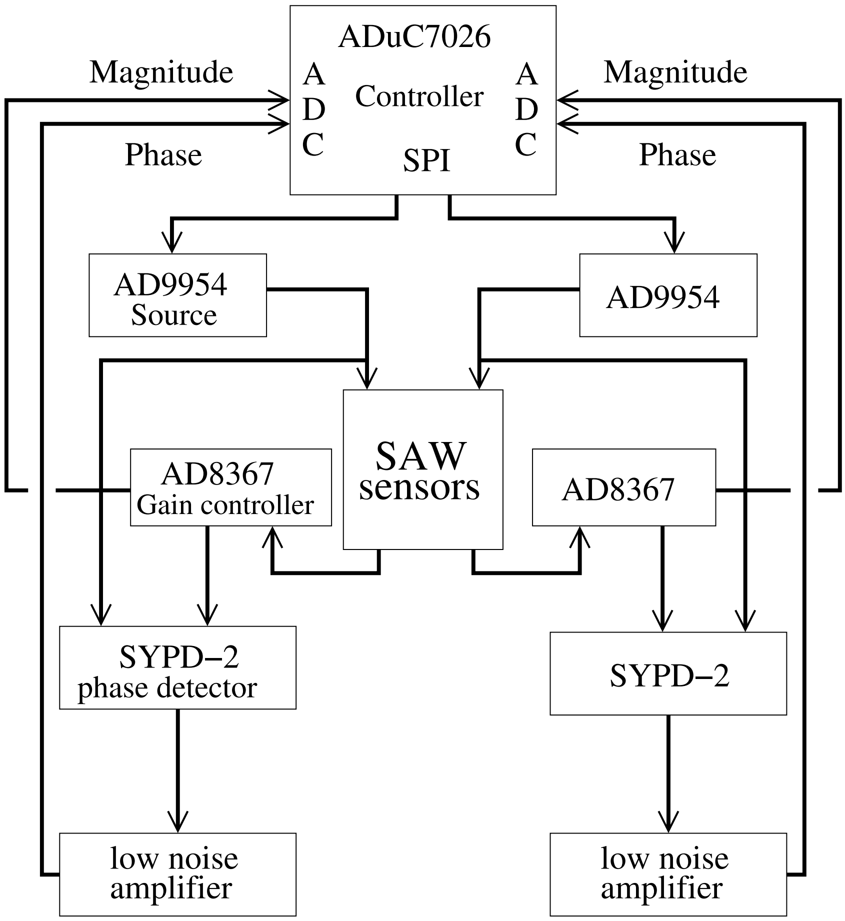

Figure 2: General diagram of the two SAW sensors interrogation electronic set-up including high accuracy functionalities using automatic gain controller AD8367 and phase detector SYPD-2 with low noise amplifier stage .

switching from one gain to another is controlled by the ADuC7026 microcontroller through an analog switch.

Fig. 4 shows the evolution of the transfer function when increasing the amplifier gain. The digitized phase measurement noise level is independent of the gain: the noise level is either due to the analog-to-digital conversion step, solely due to the unstable reference of the internal voltage used by the conversion stage, or unoptimized board layout when separating the analog and digital parts of the power supplies.

This method, which focuses on the phase measurement around the analog-to-digital converter (ADC) mid-range, yields the system to saturate if the phase shifts during the reaction, a condition which is quickly met for the highest gains. A first strategy to avoid this situation is to continuously track the phase, and to control the frequency to keep the phase close to a setpoint near the ADC mid-range. An alternative strategy requires a preliminary calibration of the phase frequency slope, to allow the phase for slowly drifting towards one of the range boundaries, and once reached, to control the frequency to bring the measurement back to the ADC mid-range.

The former method revealed effective for slowly varying signals. The frequency is recorded as the measured quantity and the phase only provides an error signal to control the efficiency of

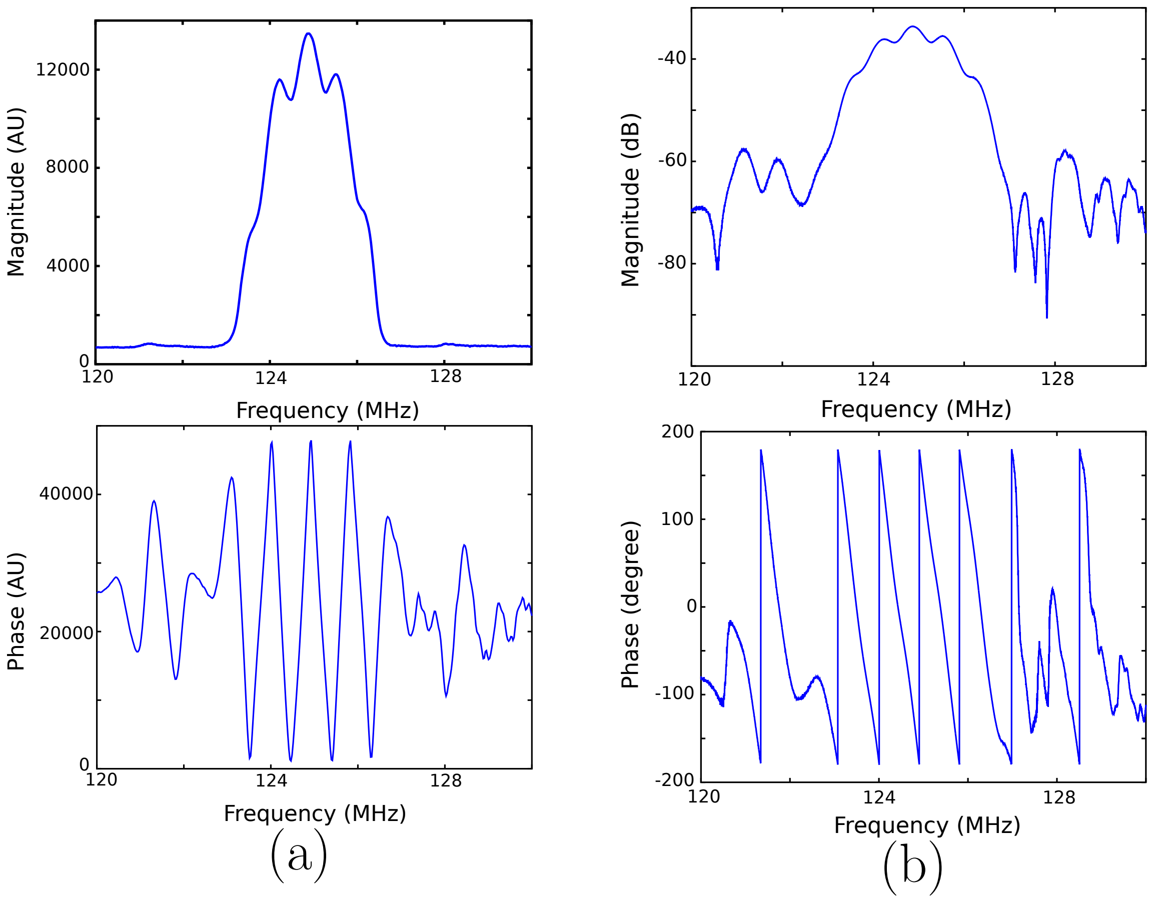

Figure 3: Magnitude (top) and phase (bottom) S_{21} characterization of a Love mode SAW delay line. Comparison between the measurement obtained using the embedded electronics (a) and Agilent Technologies E5071B commercial network analyzer (b). As opposed to a network analyzer characterization providing a phase measurement in the 0-360^o range, one can note the lack of sign information in the phase output of the AD8302, yielding phase measurements in the 0-180^o range.

the digital feedback control loop. However, the algorithm which requires phase tracking induces limits on the chemical reaction kinetics, as will be shown later (section 3).

The latter method only requires reprogramming the DDS when the phase signal comes close on to the ADC boundaries. The phase-frequency slope is characterized for each new transducer, and is solely a function of the acoustic wave velocity, which slightly changes for a given kind of acoustic waves (Rayleigh or Love) during a sensing experiment. Furthermore, this frequency-phase slope depends on the amplification gain. Therefore, an array with defined slopes is stored in the memory of the microcontroller for each kind of transducer and for each gain.

2.3 Noise level comparisons

During the coarse qualification step, the typical noise level sampling on a 16-bit range is converted to a phase standard deviation of 0.1 degree (according to a frequency standard deviation of 223 Hz for the tested sensor), at least two orders of magnitude worst than typical closed-loop oscillator noise level. The improved electronics exhibits a constant gain-independent noise level (Table 1): hence, the relative noise level decreases as the gain increases. The resulting phase noise level then corresponds to a standard deviation of 8.2×10^{-3} degree (according to

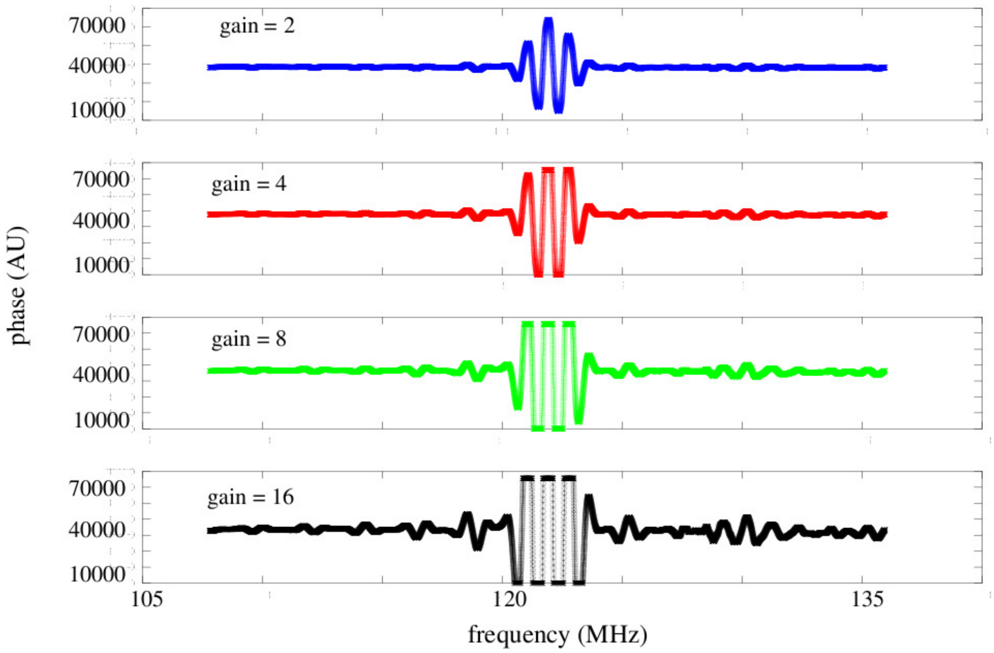

Figure 4: High resolution S_{21} phase characterization of a Love-mode SAW delay line using four different gains of the low noise amplifier stage.

a frequency standard deviation of 16 Hz for the tested sensor). This noise level is still worse than what achieved using an oscillator strategy, but as it does not depend on the operational amplifier gain and principally attributed to the ADC noise, faster sampling rates together with digital averaging and improved analog circuit layout provide paths towards improving this result. Considering a possible detection of three times the noise level this electronics provides the possibility to detect phase variation of 24.6 $\times 10^{-3}$ degree.

Table 1: Standard-deviation in bits, degree and Hz of frequency/phase measurements according to phase variation in SAW characterization using I/Q demodulator and phase detector with different low noise amplifier gains (see [10]).

	I/Q demodulator AD8302	Phase detector SYPD-2		
		gain=1	Gain=4.5	gain=17.4
standard deviation (bits)	26.3	20.3	11	30
standard deviation (degree)	0.10	0.967	0.012	0.0082
standard deviation (Hz)	222.8	195.9	23	16

3 Electro-deposition reaction monitoring

Copper electro-deposition has been used for calibrating the gravimetric sensitivity of acoustic sensors [11] exploiting an independent estimate of the deposited metal mass through the measurement of the current generated by the potentiostat [12, 13]. When using a closed loop strategy to keep the phase measurement within the measurement range of the ADC at highest gain, the fast reaction rate and large phase shift provide a challenging measurement condition for validating the phase tracking algorithms.

The generation of the potentiostat voltage driving and electro-deposition parameters (counter electrode voltage and current) are controlled and monitored by the microcontroller also driving the SAW monitoring circuits, yielding data synchronization. A typical experimental cycle is reported in Fig. 5, with a negative current indicating copper reduction (deposition on the working electrode) and a positive current indicating oxidation (copper removal from the working electrode). Reversibility is a selective criterion for implementing this experiment as it provides the means for quickly testing various acoustic phase measurement and tracking algorithm parameters. Simultaneous to the current monitoring, the acoustic phase and magnitude at fixed frequency are recorded (Fig. 6). For largest gains, as used when recording the data plotted in Fig. 6, the feedback loop on the emitted frequency to keep the phase within the measurement range of the ADC induces a phase wrapping. In fact if the phase value is near the saturation area of the ADC (below 0.2 V and above 2.3 V) The operating frequency is adjusted to get a phase value in the middle range of the ADC (Fig. 6 (top)).

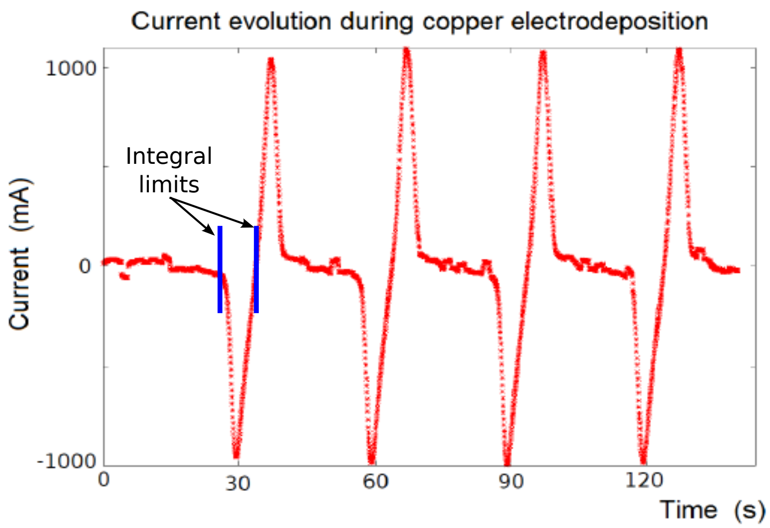

Figure 5: Current monitored during copper electro-deposition reactions and point selection defining the limit for integral calculation.

High resolution phase reconstruction is obtained by unwrapping as shown in Fig. 6. As one can see in this figure, the original 16-bit resolution has now been increased to a 17-bit resolution using the given gain of 4 at maximum gain (16), an additional 4-bit resolution improvement is obtained with no significant increase of the noise level.

The quantity of copper deposited on the sensitive surface of each device is determined by equation (3) according to the chemical reaction (4). The electro-deposition current is converted in voltage by the potentiostat and its characteristics enable the inverted conversion after the copper deposition to determine the current evolution of the chemical reaction. The time between each recorded point is fixed by the microcontroller according to 1000 points per period of 15 to 30 seconds thus changing the deposited mass on the sensor sensitive surface. To determine the deposited mass, the integral of the current during copper reduction is performed during the time delay defined as in Fig 5. Knowing sampling time and current value the deposited mass

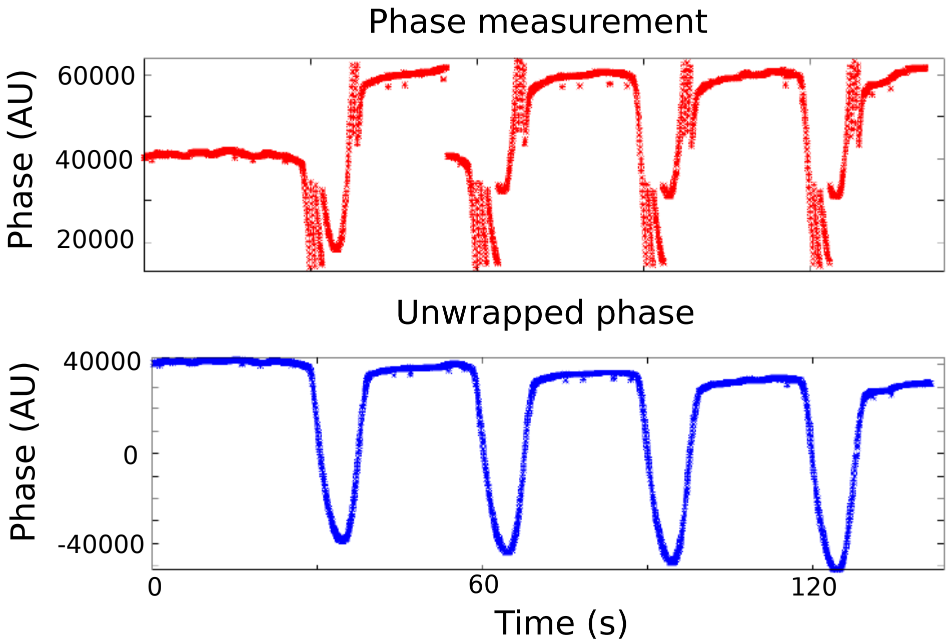

Figure 6: Recorded phase values during electro-deposition with feedback (top) and unwrapped phase information by unwrapping (bottom).

can be calculated using equation (3).

$$M_{Cu} = \frac{m_{Cu} \times \Sigma i(t)\delta t}{96440 \times n_e} \tag{3}$$

Where
M_{Cu} is the copper deposited mass (g),
m_{Cu} is the molar weight (g/mol),
$\Sigma i(t)\delta t$ the number of charge transferred during electro-deposition.
The charge of one mole of electron (C) is 96440 and
n_e the number of electrons transferred during reduction is given by (4).

$$Cu^{2+} + 2e^{-} \leftrightarrow Cu \tag{4}$$

Using this result combined with the mass-frequency dependance, relative to the Love-wave device, gravimetric senstivity is determined by using equation (5).

$$S = \frac{\Delta f}{f_0} \times \frac{A}{\Delta m} \tag{5}$$

Where
Δf is frequency shift (Hz),
f_0 the interrogation frequency (Hz),
Δm is the deposited mass (g),
A the sensitive zone area (cm^2) and
S the gravimetric sensitivity (cm^2/g).

The resulting mass sensitivity of the SAW acoustic sensor, which requires both accurate acoustic phase and potentiostat current measurements, are consistent with previous estimates:

a value of 180$\pm$20 cm^2/g is consistent with acoustic velocity gradient with respect to the guiding layer thickness from modeling [14] and with previous experimental estimates [12].

The embedded electronics is limited by the speed of phase tracking which might not be able to cope with chemical reaction exhibiting fast kinetics. Electrodeposition reaction is one example of such a fast reaction. The time of reprogramming the DDS and the measurement of the phase is of $\Delta t = 12$ ms. Considering this time and the gravimetic sensitivity measured ($S = 180$ cm^2/g) in this experiment, the maximum speed of variation of the thickness of the deposited copper on the sensing surface measured with the embedded electronic can be calculated. Our analysis is as follows:

The relationchip between the phase variation and the frequency value (used for the gravimetric sensitivity determination) is fixed by the sensor structure and determined using a frequency sweep (Fig. 3).

$$\Delta f \times \alpha = \Delta\varphi \tag{6}$$

Where
α is the relationchip constant ($bits/Hz$),

Using the equation (5) the frequency variation becomes:

$$\Delta f = S \times \frac{\Delta m}{A} \times f \tag{7}$$

Using the equation (6) and (7) $\frac{\Delta\varphi}{\Delta t}$ can be written:

$$\frac{\Delta\varphi}{\Delta t} = \frac{S \times \frac{\Delta m}{A} \times f \times \alpha}{\Delta t} \tag{8}$$

The mass variation can be express as thickness variation Δh of a layer made of a material of density ρ:

$$\frac{\Delta m}{A} = \rho \times \Delta h \tag{9}$$

hence

$$\frac{\Delta\varphi}{\Delta t} = S \times \rho \times f \times \alpha \times \frac{\Delta h}{\Delta t} \tag{10}$$

This phase variation $\Delta\varphi$ occuring during Δt must be smaller than halfrange of the analog to digital converter – or a conservative value of 32765 for a 16 bits ADC:

$$S \times \rho \times f \times \alpha \times \frac{\Delta h}{\Delta t} < \frac{halfrange}{\Delta t} \tag{11}$$

The numeric application gives a speed of increasing (or decreasing) of the thickness on the sensing area of 1.6 μm/s using the I/Q demodulator. This maximum speed is reduced to 100 nm/s using the low noise phase measurement with a gain of the amplification of 16.

4 Measurements of HBAR based sensors

As explained above, electro-deposition reaction monitoring is useful to compare gravimetric sensitivity of several sensors. The developed electronics then is used to determine the gravimetric sensitivity of acoustically-coupled HBAR [15]. This type of transducer consists of two resonators very close one an other to allow for evanescent wave coupling between the two resonators apart the electrodes.

The use of this type of resonator is motivated by its ability to provide several overtone and the possibility to read high gravimetric sensitivity in a similar approach to what was achieved using thin Film Bulk Acoustic Resonator [16, 17]. The idea then is to combine both characteristics to provide an enhanced analysis of adsorbed media compared to single mode devices. Moreover works have been done for the temperature compensation [18, 19] allowing a robust mass detection vs environmental temperature variations.

The HBAR consists of a stack of layers. A thin piezoelectric layer is used to excite bulk waves in a high quality substrate, providing a wide band multimode ray spectrum as explained in [20]. In this work, a 15 μm (YXl)/163 $LiNbO_3$ layer is used to excite pure shear waves in a AT-cut quartz substrate according to [21] . On the free surface of the quartz substrate (backside of the sensor), the sensing functional layer or working electrode on which the copper will be reversibly plated is deposited.

Based on the electrical characterization of the transducer provided by the electronics, the working frequency which (Fig. 7) is selected to correspond to a downward slope of the phase variation in the frequency sweep characterization. As previously explained, HBAR-based sensors provide several overtones and one of them is chosen here to determine the gravimetric sensitivity of the corresponding mode.

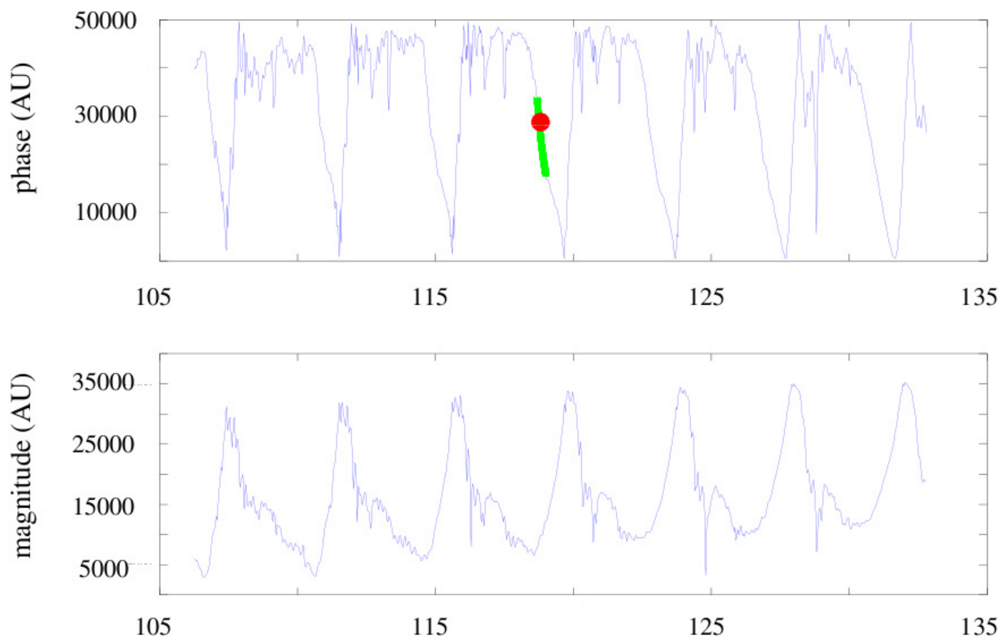

Figure 7: Magnitude (bottom) and phase (top) of the transfer function (S_{21}) of an acoustically coupled HBAR used for gravimetric measurement. Point is located at the interrogation frequency. The thick solid line represents the frequency/phase range for phase to frequency conversion.

The electronics provides raw values of phase variations related to the above-mentioned electro-deposition informations. To convert phase variations in relative frequency variations used in the equation of gravimetric sensitivity (5), a second degree polynomial fit is performed for determining the relation between raw values of phase and frequency variations. The conversion imposes to select several points whose must encompass all the values read during the electrochemical deposition corresponding to the chosen range (thick solid line in Fig. 7) around the working frequency (point). The polynomial fit is used to determine the relation between phase and frequency in the selected range to increase the number of points – up to 10000 – which define the phase value read during the experiment. A search of the closer recalculated point of phase between each recorded phase point during the reaction is performed to evaluate the effective frequency for which the conversion between phase and frequency variations is provided.

Obtaining several different results of the gravimetric sensitivity from 2.2 to 13 cm^2/g depending on the deposited mass from 1.7 to 2.6 μg emphasizes a difficulty for taking into account paramter such as viscosity and surface rougness which impact the frequency and signal magnitude as well [22, 23]. Experiments simulations have to be completed to identify the phenomena related to the frequency shift during the electrochemical deposition of copper and to improve the gravimetric sensitivity.

5 Conclusion

An approach based on synchronous detection principles using an accurate phase detector has been developed for gravimmetric surface or bulk wave sensors. An improvement by a factor 16 of the resolution of phase measurement has been demonstrated providing the possibility to detect phase variation down to 24.6 $\times 10^{-3}$ degree. The resolution gain has been achieved by reducing the system bandwidth, which is nevertheless sufficient for most chemical reaction monitoring at a few hertz sampling rate at most. This embedded frequency sweep electronics operating almost like a network analyzer combines the robustness of an open-loop strategy for assessing the operation of the sensor, and provides the resolution needed for practical gas detection applications which may correspond to sub-ppm concentration, yielding very small phase shifts (typically 100 $\times 10^{-3}$ degree).

The electronics has been developed to operate in the 60-133 MHz and 200-500 MHz ranges, allowing for testing various sensor configuration, operating points and system architecture. A particular possibility to probe various resonances of a HBAR has been developed, allowing for a wide frequency range characterization of surface phenomena. This functionality is particularly attractive for dissociating frequency-dependent effects (viscosity for instance) from more classical adsorption effects, and therefore enhanced the system accuracy and reliability.

References

[1] A. Abdelghani, J. Chovelon, N. Jaffrezic-Renault, C. Ronot-Trioli, C. Veillas, and H. Gagnaire, “Surface plasmon resonance fibre-optic sensor for gas detection,” *Sensors and Actuators B: Chemical*, vol. 39, no. 1-3, pp. 407–410, 1997.

[2] M. Benounis, N. Jaffrezic, and J. Dutasta, “Nir and optical fiber sensor for gases detection produced by transformation oil degradation,” *Sensors and Actuators A: Physical*, vol. 141, no. 1, pp. 76–83, 2008.

[3] D. Rebière, C. Dejous, J. Pistré, J. Aucouturier, C. Tiret, and R. Planade, “Acoustic wave devices to measure gas flow: comparison between surface acoustic wave (saw) and shear horizontal acoustic plate mode (sh-apm) oscillators,” *Sensors and Actuators A: Physical*, vol. 42, no. 1-3, pp. 384–388, 1994.

[4] F. Herrmann, M. Weihnacht, and S. Büttgenbach, “Properties of shear-horizontal surface acoustic waves in different layered quartz–sio¡ sub¿ 2¡/sub¿ structures,” *Ultrasonics*, vol. 37, no. 5, pp. 335–341, 1999.

[5] E. Gizeli, “Study of the sensitivity of the acoustic waveguide sensor,” *Analytical chemistry*, vol. 72, no. 24, pp. 5967–5972, 2000.

[6] J. Du and G. Harding, “A multilayer structure for love-mode acoustic sensors,” *Sensors and Actuators A: Physical*, vol. 65, no. 2-3, pp. 152–159, 1998.

[7] J. Rosenbaum, *Bulk acoustic wave theory and devices.* Artech House Boston and London, 1988, vol. 376.

[8] M. Vanotti, V. Blondeau-Patissier, D. Rabus, S. Ballandras, M. Chkounda, J. Barbe, and J. Rauch, “Development of acoustic devices functionalized with cobalt corroles or metalloporphyrines for the detection of carbon monoxide at low concentration,” *Sensors and Transducers*, no. 14-1, pp. 197–211, 2012.

[9] E. Rubiola, *Phase noise and frequency stability in oscillators*, ser. The Cambridge RF and microwave engineering series. Cambridge University Press, Nov. 2008. [Online]. Available: http://hal.archives-ouvertes.fr/hal-00344308

[10] “supplementary material.”

[11] G. Sauerbrey, “Verwendung von schwingquarzen zur wägung dünner schichten und zur mikrowägung,” *Zeitschrift für Physik A Hadrons and Nuclei*, vol. 155, no. 2, pp. 206–222, 1959.

[12] J.-M. Friedt, L. Francis, K.-H. Choi, and A. Campitelli, “Combined atomic force microscope and acoustic wave devices: Application to electrodeposition,” *J. Vac. Sci. Tech. A*, vol. 21, no. 4, p. 1500, 2003.

[13] A. Rowe, A. Bonham, R. White, M. Zimmer, R. Yadgar, T. Hobza, J. Honea, I. Ben-Yaacov, and K. Plaxco, “Cheapstat: An open-source,“do-it-yourself” potentiostat for analytical and educational applications,” *PloS one*, vol. 6, no. 9, p. e23783, 2011.

[14] L. Francis, J.-M. Friedt, R. D. Palma, P. Bertrand, and A. Campitelli, “Influence of electromagnetic interferences on the gravimetric sensitivity of surface acoustic waveguides,” *Sensors and Actuators A*, vol. 123-124, pp. 360–369, 2005.

[15] D. Gachon, T. Baron, G. Martin, E. Lebrasseur, E. Courjon, F. Bassignot, and S. Ballandras, “Laterally coupled narrow-band high overtone bulk wave filters using thinned single crystal lithium niobate layers.” IFCS-EFTF, May 2011.

[16] M. Nirschl, A. Blüher, C. Erler, B. Katzschner, I. Vikholm-Lundin, S. Auer, J. Vörös, W. Pompe, M. Schreiter, and M. Mertig, “Film bulk acoustic resonators for dna and protein detection and investigation of in vitro bacterial s-layer formation,” *Sensors and Actuators A: Physical*, vol. 156, no. 1, pp. 180–184, 2009.

[17] W. Xu, X. Zhang, S. Choi, and J. Chae, “A high-quality-factor film bulk acoustic resonator in liquid for biosensing applications,” *Microelectromechanical Systems, Journal of*, vol. 20, no. 1, pp. 213–220, 2011.

[18] T. Baron, D. Gachon, G. Martin, S. Alzuaga, D. Hermelin, J. Romand, and S. Ballandras, “Temperature compensated radio-frequency harmonic bulk acoustic resonators,” in *Frequency Control Symposium (FCS), 2010 IEEE International*. IEEE, 2010, pp. 652–655.

[19] H. Yu, W. Pang, H. Zhang, and E. Kim, “Ultra temperature-stable bulk-acoustic-wave resonators with sio2 compensation layer,” *Ultrasonics Ferroelectrics and Frequency Control IEEE Transactions on*, vol. 54, no. 10, pp. 2102–2109, 2007.

[20] K. Lakin, G. Kline, and K. McCarron, “High-q microwave acoustic resonators and filters,” *Microwave Theory and Techniques, IEEE Transactions on*, vol. 41, no. 12, pp. 2139–2146, 1993.

[21] T. Baron, D. Gachon, G. Martin, S. Alzuaga, D. Hermelin, J. Romand, and S. Ballandras, “Temperature compensated radio-frequency harmonic bulk acoustic resonators,” in *Frequency Control Symposium (FCS), 2010 IEEE International*. IEEE, 2010, pp. 652–655.

[22] M. Vellekoop, “Acoustic wave sensors and their technology,” *Ultrasonics*, vol. 36, no. 1, pp. 7–14, 1998.

[23] L. Elvira-Segura, “Acoustic wave dispersion in a cylindrical elastic tube filled with a viscous liquid,” *Ultrasonics*, vol. 37, no. 8, pp. 537–547, 2000.